Analytic Solution for a Cruising Plane Change Maneuver

Richard T. Cervisi*
Rockwell International, Downey, California

The analytical solution for a cruising plane change maneuver predicts the plane change during a constant altitude, velocity, and angle-of-attack turn. Thrust balances drag and bank angle varies with mass to provide inplane equilibrium. The solution predicts the impulsive plane change and corrections for finite arc length and noncircular velocity. Test cases show that inclination change predictions approximate numerically integrated results by 1%. The accuracy of predicting changes in longitude of the ascending node depends on the initial inclination, with prediction errors of 1% for polar orbits. The solution's derivatives provide the initial argument of latitude, velocity, and angle of attack that maximize the plane change.

Nomenclature

A_R = radial perturbation acceleration
A_S = perturbation acceleration perpendicular to A_R and in direction of increasing true anomaly
A_W = perturbation acceleration perpendicular to A_R and A_S
a = semimajor axis
C = $(Vc^2 - V^2)/r/[L + T\sin(\alpha)]$
C_D = drag coefficient
C_{DO} = drag coefficient at zero lift
$C_{L\alpha}$ = lift coefficient slope
C_{LO} = lift coefficient at zero angle of attack
C_L = lift coefficient
D = drag
Ep = aeropropulsive efficiency $[(L/D)\cos(\alpha) + \sin(\alpha)]$
e = eccentricity
g = gravitational acceleration at the earth's surface
h = altitude and angular momentum
I_{sp} = specific impulse
i = inclination
i_0 = initial inclination
Δi = change in inclination
K = constant in drag coefficient function
L = lift
m = mass
$\dot{m}$ = mass flow rate $[D/gI_{sp}\cos(\alpha)]$
m_n = mass at nodal crossing
m_0 = initial mass
n = mean motion $(\sqrt{\mu/a^3})$ and exponent in drag coefficient function
p = semiparameter
r = radial distance from center of earth
S = aerodynamic reference area
T = thrust
t = time
u = argument of latitude
u_0 = initial argument of latitude
u' = rate of change of u with respect to mass
V = velocity
V_c = circular orbit velocity
W_0 = initial weight
W_f = final weight
α = angle of attack
μ = gravitational constant
ν = true anomaly
σ = bank angle
Ω = longitude of the ascending node
$\Delta\Omega$ = change in longitude of the ascending node
ω = argument of perigee

Introduction

RECENT studies of space sortie vehicles have revived interest in synergetic plane change maneuvers.[1-4] The moderate to high lift to drag ratio of these vehicles could be used to change inclination or longitude of the ascending node at a ΔV expenditure that is smaller than that of an equivalent exoatmospheric maneuver. The plane change capability could shorten the time needed to reach multiple reconaissance targets on a single orbital mission, reduce the time needed to return to base from orbit, and complicate tracking of the sortie vehicle. Effecting rendezvous with satellites in different orbital planes and avoiding flight over hostile territory are other possible uses of the plane change capability.

Reference 5 classifies the synergetic plane change as either an aeroglide or an aerocruise. The aeroglide uses propulsive forces for reentry and reboost and the plane change is done with aerodynamic lift. The aerocruise also uses propulsive forces for reentry and reboost, but both propulsive and aerodynamic forces are used to maintain a constant altitude and velocity turn.

In the mid 1960's, Lau[6] and Clauss and Yeatman[7] showed how practical heat rate limits could constrain the plane change provided by a synergetic maneuver. Clauss and Yeatman compared the performance of the aeroglide and aerocruise subject to heat rate limits. They found that the plane change reduction caused by the heat rate limit is "more severe for the aeroglide than for the aerocruise mode of the maneuver, indicating that the aerocruise is the superior mode."[7]

Aerocruise has the additional advantage of simplicity. The flight regime, dynamic pressure, and reference heat rate are constant during the maneuver. If the angle of attack is fixed, the vehicle's aerodynamic coefficients, pressure distribution, and heating environment are also constant, and the bank angle is a simple function of the mass. These features facilitate the design and control of the maneuver and the vehicle.

In recent years, numerical optimization techniques have been used to study synergetic plane change maneuvers.[8-11] Numerical and preliminary design studies are facilitated by analytic solutions. These solutions can narrow the scope of detailed trajectory optimization studies, provide estimates of ΔV requirements and environmental loads, and determine the design parameters (lift to drag, wing loading, and thrust requirement) of a conceptual vehicle.

Analytic solutions for aeroglide are available in Refs. 12 and 13. Analytic solutions for aerocruise in Refs. 5 and 14 are

Presented as Paper 83-2095 at the AIAA Atmospheric Flight Conference, Gatlinburg, Tenn., Aug. 15-17, 1983; received Aug. 25, 1983; revision received March 2, 1984.

*Member of Technical Staff IV, Advanced Programs, Shuttle Orbiter Division. Member AIAA.

based on the minor circle turn and the perturbation from a conic orbit, respectively. Both solutions assume constant mass, angle of attack, and bank angle; the latter solution is restricted to a 90-deg bank angle and orbital velocities.

The analytic solution presented here predicts the plane change during a constant angle-of-attack cruising turn. The maneuver is depicted in Fig. 1. The bank angle varies with the mass to provide vertical equilibrium and constant altitude, and thrust cancels drag to maintain constant velocity. The solution applies just to the powered turn and does not address the deboost from orbit or the reboost to orbit segments.

The solution's derivation is presented in the following section, which includes a discussion of the approximations that led to the analytic solution. It is followed by a comparison of the solution's plane change predictions with the results of numerically integrated trajectories. Derivatives of the solution with respect to initial argument of latitude, velocity, and angle of attack are presented in the Appendix.

Derivation

Basic Equations

The solution is derived from the variation of the orbital elements, perturbation forces, and equation for the mass. It assumes a spherical and nonrotating Earth. The general variations of orbital elements are presented in Table 1. These equations are taken from Refs. 15 and 16. If the perturbation forces are zero, the equations describe a conic orbit. The argument of latitude is chosen to specify angular position in the orbital plane because the variations of inclination and longitude of the ascending node are functions of this angle.

During aerocruise, the flight path angle is zero. This means the true anomaly is 0 or 180 deg and the first terms in the equation for $\mathrm{d}a/\mathrm{d}t$ and $\mathrm{d}e/\mathrm{d}t$ vanish. Also, note that

$$na^2\frac{\sqrt{1-e^2}}{r}=V \qquad (1)$$

The perturbation force diagram is illustrated in Fig. 2. These are all the forces on the vehicle except gravity. The perturbation accelerations along each axis follow directly from the figure:

$$A_R=\frac{[L+T\sin(\alpha)]\cos(\sigma)}{m} \qquad (2)$$

$$A_S=\frac{T\cos(\alpha)-D}{m}=0 \qquad (3)$$

$$A_W=\frac{[(L+T\sin(\alpha)]\sin(\sigma)}{m} \qquad (4)$$

The perturbation acceleration along the R axis can also be expressed as

$$A_R=\frac{Vc^2-V^2}{r}=\frac{\mu}{r^2}-\frac{\mu(1-e)}{r^2}=\frac{\mu e}{r^2} \qquad (5)$$

for aerocruise at subcircular and circular velocities.

The equation for the mass is

$$\frac{\mathrm{d}m}{\mathrm{d}t}=-\dot{m} \qquad (6)$$

The mass flow rate is constant since the altitude, velocity, and angle of attack are constant.

Using Eqs. (1), (3), and (5), the general variations are reduced to the variation of the orbital elements for aerocruise. These equations appear on the right side of Table 1. The semimajor axis and the eccentricity are unchanged by the maneuver. The variations of the arguments of perigee and latitude are identical. The only remaining perturbation acceleration is the component perpendicular to the orbital plane. To determine the plane change (Δi or $\Delta\Omega$), the equation for the argument of latitude must be integrated. This step is discussed in the following section.

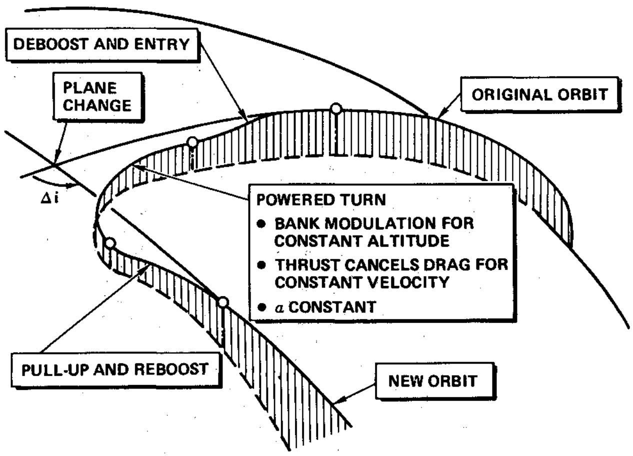

Fig. 1 Schematic diagram of aerocruise plane change.

Table 1 Reduction of the general variation of the orbital elements to those for aerocruise

Element	General variation of orbital elements	Variation of elements for aerocruise
$\frac{\mathrm{d}a}{\mathrm{d}t}$	$\frac{2e\sin(\nu)}{n\sqrt{1-e^2}}A_R+\frac{2a\sqrt{1-e^2}}{nr}A_S$	0
$\frac{\mathrm{d}e}{\mathrm{d}t}$	$\frac{\sqrt{1-e^2}\sin(\nu)}{na}A_R+\frac{\sqrt{1-e^2}}{na^2e}\left[\frac{a^2(1-e^2)}{r}-r\right]A_S$	0
$\frac{\mathrm{d}i}{\mathrm{d}t}$	$\frac{r\cos(u)}{na^2\sqrt{1-e^2}}A_W$	$\frac{\cos(u)}{V}A_W$
$\frac{\mathrm{d}\Omega}{\mathrm{d}t}$	$\frac{r\sin(u)}{na^2\sqrt{1-e^2}\sin(i)}A_W$	$\frac{\sin(u)}{V\sin(i)}A_W$
$\frac{\mathrm{d}\omega}{\mathrm{d}t}$	$-\frac{\sqrt{1-e^2}\cos(\nu)}{nae}A_R+\frac{p}{eh}\left[\sin(\nu)\left(1+\frac{1}{1+e\cos(\nu)}\right)\right]A_S$ $-\frac{r\cot(i)\sin(u)}{na^2\sqrt{1-e^2}}A_W$	$\frac{V}{r}-\frac{\sin(u)}{V\tan(i)}A_W$
$\frac{\mathrm{d}u}{\mathrm{d}t}$	$\frac{na^2\sqrt{1-e^2}}{r^2}-\frac{r\cot(i)\sin(u)}{na^2\sqrt{1-e^2}}A_W$	$\frac{V}{r}-\frac{\sin(u)}{V\tan(i)}A_W$

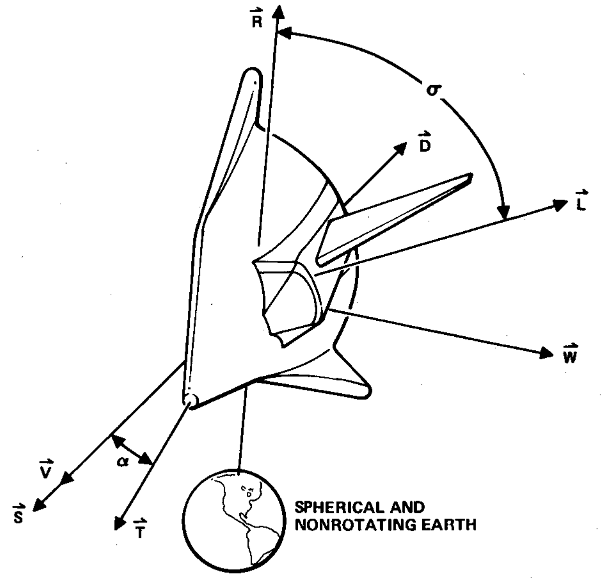

Fig. 2 Perturbation force diagram for aerocruise in the RSW coordinate system.

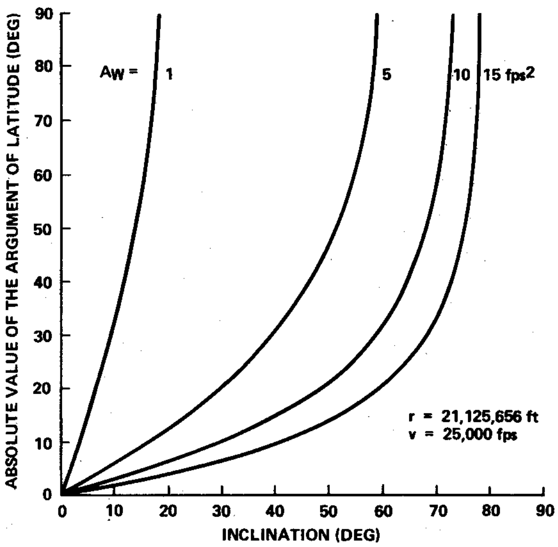

Fig. 3 Conditions when the argument of latitude perturbation can be neglected.

Solving for the Argument of Latitude

The variation of the argument of latitude for aerocruise is

$$\frac{du}{dt} = \frac{V}{r} - \frac{\sin(u)}{V\tan(i)}A_W \tag{7}$$

This equation is easily integrated if the second term can be neglected. To study this possibility, assume the second term can be neglected if it is an order of magnitude smaller than the first term. The relationship between argument of latitude, inclination, and perturbation acceleration for which this situation will occur is mathematically stated as

$$u \leq \sin^{-1}\left[\frac{(0.1)V^2\tan(i)}{rA_W}\right] \tag{8}$$

for arguments of latitude that are between plus and minus 90 deg.

Equation (8) is plotted in Fig. 3 for representative values of velocity, altitude, and acceleration. The acceleration of 15 fps^2 in the figure is associated with a heat rate that is higher than a typical sortie vehicle can withstand.

The figure indicates that the second term of Eq. (7) can be neglected at all values of the argument of latitude if the inclination is near 90 deg. The variation of the inclination in Table 1 shows that an aerocruise to change inclination must occur near the ascending or descending nodes ($u = 0$ or 180 deg) to be effective. For this maneuver, the second term of Eq. (7) can be neglected over a wider range of inclinations. In addition, efficient maneuvers that change inclination are evenly spaced about the node. Since the second term in Eq. (7) changes sign at the node, this term's integrated contribution to changing the argument of latitude is small.

These considerations make it plausible to neglect the second term in Eq. (7); this approximation is adopted in the subsequent development. Judging from Fig. 3, the prediction of inclination change based on this approximation will be accurate over a wider range of initial inclinations than will the prediction of the change in longitude of ascending node. The consequences of this approximation are further explored when the predictions of the analytic solution are compared to numeric results in a later section.

With this approximation and with Eq. (6) to change the independent variable from time to mass, the variation of the argument of latitude becomes

$$\frac{du}{dm} = -\frac{V}{r\dot{m}} = -u' \tag{9}$$

This equation is easily integrated to give

$$u = u'(m_0 - m) + u_0 \tag{10}$$

The argument of latitude is linear with respect to mass and time.

Integration of the variation of inclination, which is discussed in the following section, is facilitated by expanding a term of the equation for this variation about the mass at the node. If this point is assumed to be the ascending node ($u = 0$ deg), Eq. (10) provides a value for this mass

$$m_n = \frac{u_0 + u'm_0}{u'} \tag{11}$$

The equation for the argument of latitude becomes

$$u = u'(m_n - m) \tag{12}$$

Solving for the Change in Inclination

After changing the independent variable to the mass and using Eq. (12) for the argument of latitude, the variation of inclination for aerocruise is

$$\frac{di}{dm} = -\frac{\cos[u'(m_n - m)]}{V}\frac{A_W}{\dot{m}} \tag{13}$$

The combination $A_W/\dot{m}$ can also be expressed as a function of the mass by using Eqs. (3), (4), and (5). The result is

$$\frac{A_W}{\dot{m}} = gI_{sp}Ep\frac{\sqrt{1-(Cm)^2}}{m} \tag{14}$$

where

$$Cm = \cos(\sigma) \tag{15}$$

To facilitate the subsequent integration, the square root expression in Eq. (14) can be approximated with the binomial expansion. The approximation is

$$\sin(\sigma)=\sqrt{1-(Cm)^2}\approx 1-\frac{(Cm)^2}{2} \tag{16}$$

The approximation is accurate to within 1% for bank angles between 60 and 120 deg. It is intuitively reasonable because the turning force is provided by the banked lift and thrust vectors and this force is maximized at a 90-deg bank angle.

Combining Eqs. (13), (14), and (16) gives the variation of the inclination with respect to the mass:

$$\frac{\mathrm{d}i}{\mathrm{d}m}=-\frac{gI_{sp}Ep}{V}\frac{2-(Cm)^2}{2m}\cos[u'(m_n-m)] \tag{17}$$

The integral of this differential equation provides the inclination change during aerocruise. The integral is

$$\Delta i=-\frac{gI_{sp}Ep}{V}\int_{m_0}^{m}\left(\frac{\cos[u'(m_n-m)]}{m}-\frac{C^2m\cos[u'(m_n-m)]}{2}\right)\mathrm{d}m \tag{18}$$

The integrand contains two terms that can be integrated separately and their results combined. Before proceeding, it should be noted that the first term accounts for the distribution of the maneuver about the node with the bank angle at 90 deg, while the second term accounts for bank angles other than 90 deg.

Taking the second term first and integrating by parts gives

$$\frac{C^2}{2}\int_{m_0}^{m}m\cos(u'(m_n-m))\,\mathrm{d}m=\frac{1}{2}\left(\frac{C}{u'}\right)^2\times[u'(m_0\sin(u'(m_n-m))-m\sin(u'(m_n-m)))-\cos(u'(m_n-m_0))+\cos(u'(m_n-m))] \tag{19}$$

The argument of the sine and cosine functions in this equation is either the initial or final argument of latitude. After expanding the squared expression, Eq. (19) becomes

$$\frac{C^2}{2}\int_{m_0}^{m}m\cos(u'(m_n-m))\,\mathrm{d}m=\frac{1}{2}\left(\frac{Vc^2-V^2}{gI_{sp}EpV}\right)^2\times(u'(m_0\sin(u_0)-m\sin(u)-\cos(u_0)+\cos(u)) \tag{20}$$

This equation is zero if the aerocruise is done at circular orbit speeds and a 90-deg bank angle.

The first term of Eq. (18) can be integrated if the cosine function is expanded in a Taylor series. The mass at the node is the best point to expand around because an efficient aerocruise to change inclination will take place about the node. The integral becomes

$$\int_{m_0}^{m}\frac{\cos(u'(m_n-m))}{m}\mathrm{d}m=\int_{m_0}^{m}\left(\frac{1}{m}-\frac{u'^2}{2!}\frac{(m-m_n)^2}{m}+\frac{u'^4}{4!}\frac{(m-m_n)^4}{m}+\cdots\right)\mathrm{d}m \tag{21}$$

The integral of the first term is obvious. The other terms can be integrated with the aid of Ref. 17. The general result is

$$\frac{u'^k}{k!}\int_{m_0}^{m}\frac{(m-m_n)^k}{m}\mathrm{d}m=\frac{u'^k}{k!}\left(-m_n^k\ln\left(\frac{m_0}{m}\right)+\sum_{j=1}^{k}(-1)^j\frac{m_n^{k-j}((m-m_n)^j-(n_0-m_n)^j)}{jm_n^j}\right) \tag{22}$$

With this result, the integral is

$$\int_{m_0}^{m}\frac{\cos(u'(m_n-m))}{m}\mathrm{d}m=-\ln\left(\frac{m_0}{m}\right)+\sum_{k=1}^{\infty}(-1)^k\frac{(u'm_n)^{2k}}{(2k)!}\left[-\ln\left(\frac{m_0}{m}\right)+\sum_{j=1}^{2k}(-1)^j\frac{(m-m_n)^j-(m_0-m_n)^j}{jm_n^j}\right] \tag{23}$$

A simplification is possible by recognizing that the second summation is part of the Taylor series for the natural log of the mass ratio expanded about the node. With this simplification and some rearrangement to recover the argument of latitude, the integral is

$$\int_{m_0}^{m}\cos\frac{(u'(m_n-m))}{m}\mathrm{d}m=-\ln\left(\frac{m_0}{m}\right)+\sum_{k=1}^{\infty}\frac{(-1)^k}{(2k)!}\sum_{j=2k+1}^{\infty}(u'm_n)^{2k-j}\frac{u^j-u_0^j}{j} \tag{24}$$

The analytic solution for the change in inclination during aerocruise is obtained by combining equations (18), (20), and (24). The solution is

$$\Delta i=\frac{gI_{sp}Ep}{V}\left[\ln\left(\frac{m_0}{m}\right)+\sum_{k=1}^{\infty}\frac{(-1)^k}{(2k)!}\sum_{j=2k+1}^{\infty}(u'm_n)^{2k-j}\times\frac{u^j-u_0^j}{j}+\frac{1}{2}\left(\frac{Vc^2-V^2}{gI_{sp}EpV}\right)^2(u'(m_0\sin(u_0)-m\sin(u))-\cos(u_0)+\cos(u))\right] \tag{25}$$

The argument of latitude is given by Eq. (12). The first term in this solution gives the plane change if the maneuver could be done impulsively, the second term accounts for the distribution of the maneuver about the node, and the third term accounts for the components of lift and thrust that must be used to maintain vertical equilibrium at velocities other than circular orbit velocity.

The contribution of each term to the change in inclination for a typical sortie vehicle is depicted in Fig. 4. The sortie vehicle is described in a following section. The impulsive (first) term dominates the other two terms, which are both negative. The figure also shows how the inclination change varies with the initial argument of latitude. The third term varies by just 0.4 deg over the 60 deg initial argument of latitude range. The optimum argument of latitude is the value that minimizes the plane change loss caused by the distribution of the maneuver about the node (second term).

Also note that the plane change is proportional to the aeropropulsive efficiency (Ep) and not lift to drag ratio. In the mid 1960's, Parsons[14] reported the same result for the aerocruise maneuver he studied.

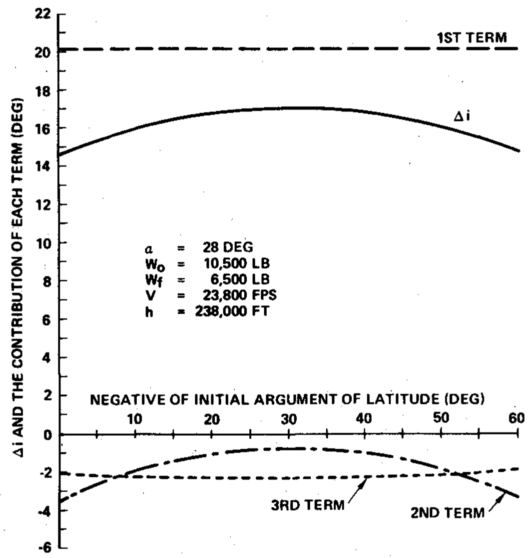

Fig. 4 Effect of the initial argument of latitude on the inclination change and on the contribution of each term of the solution.

Solving for the Change in Longitude of the Ascending Node

The variations of inclination and longitude of the ascending node for aerocruise in Table 1 indicate that concentrating the maneuver evenly about the orbit apex ($u = 90$ or 270 deg) will change the longitude of the ascending node, and since the variation of the inclination changes sign at an orbit apex, the maneuver will leave the inclination unchanged. Assuming the inclination remains constant and treating the argument of latitude in Eq. (25) as the angular displacement about the orbit apex, the change in longitude of the ascending node is given by

$$\Delta\Omega = \frac{\Delta i}{\sin(i)} \tag{26}$$

Comparison with Numerical Results

Assumptions Behind Comparison

The usefulness of the analytic solution depends on its accuracy. This section compares the plane change predictions of the analytic solution with the results of numerically integrated trajectories. The program to optimize simulated trajectories (POST) was used for these comparisons. The POST simulations used a nonrotating spherical Earth to match the assumptions behind the analytic solution.

The vehicle in this comparison is the maneuverable reentry research vehicle (MRRV).[11] Its characteristics are summarized in Table 2 and Fig. 5, and are typical of the sortie vehicles currently under investigation. The 3,000°R temperature limit behind the nose sets the maximum heat rate, which is provided by the cruise condition selected for the comparison: velocity, 23,800 fps and altitude, 238,000 ft. Figure 5 shows that the best aeropropulsive efficiency is 8% higher than the best lift to drag ratio and that the difference is greater at higher angles of attack. This characteristic is important[11] because high lift coefficients are desired to concentrate the maneuver about the node (or the apex). A 28-deg angle of attack is used in the comparison because it provides the largest plane change capability.

The initial argument of latitude in the comparison is 30.9 deg before the nodal or apex crossing. As Fig. 4 shows, this angle provides the largest plane change capability for the selected cruise condition and angle of attack.

Inclination Comparison

The analytic solution predicts a change in inclination of 17.02 deg. As illustrated in Fig. 6, the POST simulation gives a 16.83-deg change in inclination for initial inclinations from 0 to 90 deg. The difference is 1.1% and it is caused by the approximation made in Eq. (16) for the sine of the bank angle. The bank angle and the approximation error during the maneuver are illustrated in Fig. 7. As the bank angle varies from 52.4 to 67.8 deg, the error in the approximation varies from 2.7 to 0.3%.

The prediction of the change in inclination is not affected by the other approximation used to derive the solution, i.e., neglecting the perturbative variation of the argument of latitude. Figure 8 shows the solution and POST gives a linear variation of the argument of latitude at a 90-deg initial inclination. At a 5-deg initial inclination, the actual variation of the argument of latitude is nonlinear with respect to mass and time, but since the perturbative variation of this angle changes sign at the nodal crossing [see Eq. (7)], the net variation is the same as the solution's prediction.

Longitude of the Ascending Node Comparison

The accuracy of the predicted change in longitude of the ascending node depends on the initial inclination. Figure 6 shows this effect. For a 90-deg initial inclination, the solution differs from the POST simulation by 1.1%. For a 45-deg initial inclination, the error is 4%, and for a 15-deg initial inclination, the error is 33.4%.

Equation (7) and Fig. 8 show the cause of these errors. As the initial inclination decreases, the perturbative variation of the argument of latitude in Eq. (7) becomes more important. At the orbit apex in a 15-deg inclination orbit, it is 90% of the unperturbed variation, and unlike an aerocruise for changing the inclination, the perturbative variation of the argument of latitude does not change sign during the maneuver. The predicted and actual values of the argument of latitude become

Table 2 Summary of MRRV characteristics

Parameter	Value
Initial mass	10,500 lbm
Propellant available for aerocruise	4,000 lbm
Aerodynamic reference area	125 ft^2
Maximum lift to drag	2.30
Maximum *Ep*	2.48
Thrust	≤ 3,300 lbf
Specific impulse	290 s
Temperature limit	3,000°R

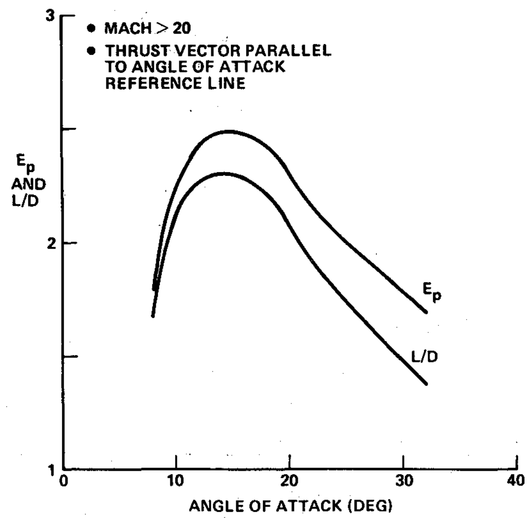

Fig. 5 Comparison of aerodynamic and aeropropulsive efficiency of the maneuverable reentry research vehicle.

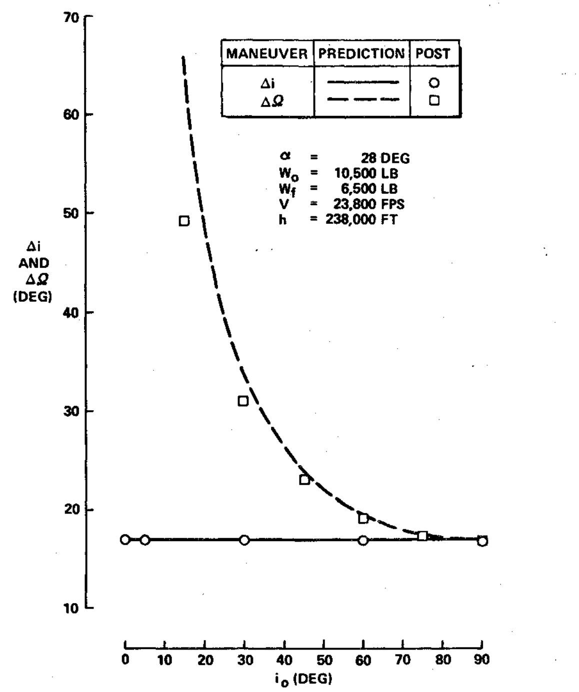

Fig. 6 Comparison of the predicted and the numerically integrated plane change angles vs the initial inclination.

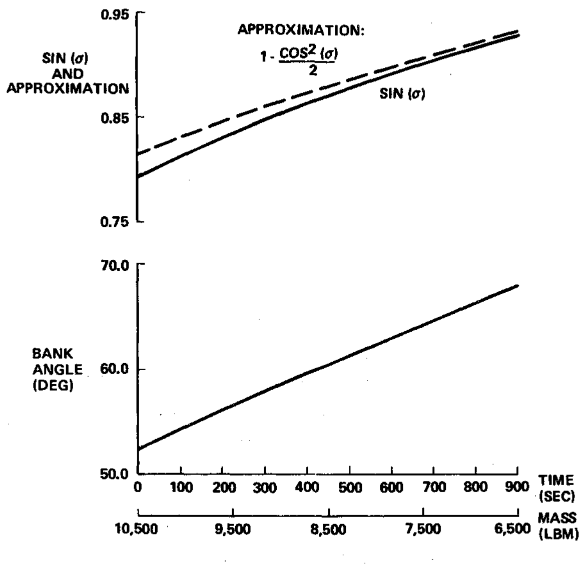

Fig. 7 Bank angle profile and the error caused by the approximation for the sine of the bank angle.

more divergent and the predicted change in longitude of the ascending node becomes more inaccurate.

Figure 9 shows that as the initial inclination decreases, the approximation of constant inclination during an aerocruise to change longitude of ascending node becomes increasingly in error. This error is also caused by the divergence of the actual and predicted values of the argument of latitude.

Conclusions

An analytic solution has been derived for a cruising plane change maneuver. The solution contains three terms that describe the three components of the maneuver: impulsive plane change, plane change loss caused by the distribution of the maneuver about the node or apex, and plane change loss caused by the components of lift and thrust that are required to maintain vertical equilibrium. The solution also shows the

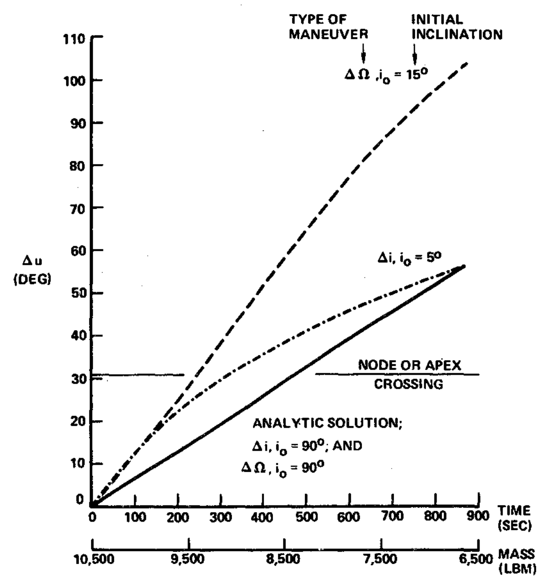

Fig. 8 Effect of the initial inclination on the change in argument of latitude during the plane change maneuver.

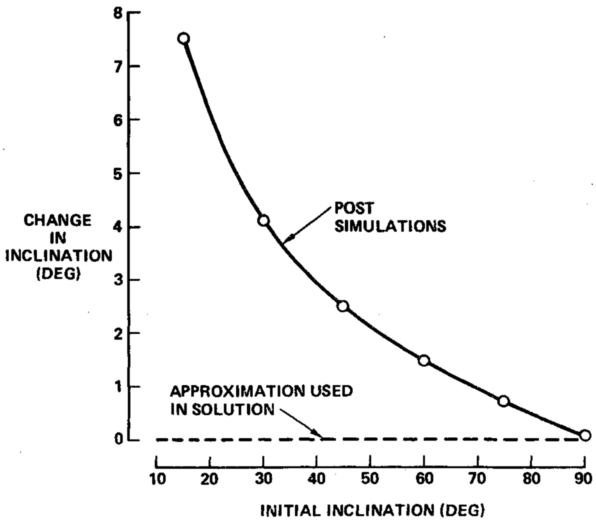

Fig. 9 Actual and approximate change in inclination during an aerocruise to change longitude of the ascending node.

plane change is proportional to the aeropropulsive efficiency and not the lift to drag ratio.

A comparison of the solution's plane change predictions with the results of numerically integrated trajectories over a spherical nonrotating earth shows that the solution predicts with 1% error a typical sortie vehicle's capability to change inclination. In addition, the comparison shows the accuracy of the predicted change in longitude of the ascending node depends on the initial inclination, with prediction errors of 1 percent for polar orbits.

Appendix

Although the derivatives of the inclination change with respect to the argument of latitude, velocity, and angle of attack are lengthy expressions, they are readily derived from Eq. (25). The intermediate derivatives required to evaluate the derivatives with respect to the inclination change are presented in Table A-1. Lift and drag coefficient functions must be assumed to evaluate the derivatives with respect to the

Table A1 Intermediate derivatives

Variable	$\frac{d}{du_0}$	$\frac{d}{dV}$	$\frac{d}{d\alpha}$
u'	0	$-\frac{u'}{V}$	$-u'\left(\tan(\alpha)+\frac{nkC_L^{n-1}}{C_0}C_{L_\alpha}\right)$
m_n	$\frac{1}{u'}$	$\frac{u_0}{u'V}$	$-\frac{u_0}{u'^2}\frac{du'}{d\alpha}$
u	1	$\frac{u_0-u}{V}$	$(m_0-m)\frac{du'}{d\alpha}$
$\frac{Vc^2-V^2}{V^2}$	0	$-\frac{Vc^2+V^2}{V^2}$	0
$\frac{L}{D}$	0	0	$\frac{\left(C_{D_0}+(1-n)kC_L^n\right)}{C_D^2}C_{L_\alpha}$
Ep	0	0	$\left(1+\frac{d(L/D)}{d\alpha}\right)\cos(\alpha)-\frac{L}{D}\sin(\alpha)$

angle of attack. The functions used in this evaluation are

$$C_L = C_{L_0} + C_{L_\alpha}\cdot\alpha \tag{A1}$$

$$C_D = C_{D_0} + KC_L^n \tag{A2}$$

The derivatives of the inclination change are presented in a format that shows the common expressions between each equation. This format also facilitates programming the equations on a handheld or desktop calculator. The derivatives are

$$\frac{d\Delta i}{du_0} = \frac{A}{m_n}\frac{dm_n}{du_0} + B + \frac{1}{2}\left(\frac{Vc^2-V^2}{gI_{sp}EpV}\right)^2 C \tag{A3}$$

$$\frac{d\Delta i}{dV} = \frac{gI_{sp}Ep}{V}\left[\left(\frac{m_0}{m_n}A + D + \frac{1}{2}\left(\frac{V_c^2-V^2}{gI_{sp}EpV}\right)^2\right.\right.$$
$$\left.\left.\times(E+F)\right)\frac{1}{u'}\frac{du'}{dV} - \frac{V_c^4-V^4}{(gI_{sp}EpV)^2}\frac{G}{V}\right] - \frac{\Delta i}{V} \tag{A4}$$

and

$$\frac{d\Delta i}{d\alpha} = \frac{\Delta i}{Ep}\frac{dEp}{d\alpha} + \frac{gI_{sp}Ep}{V}$$
$$\times\left[\left(\frac{m_0}{m_n}A + D + \frac{1}{2}\left(\frac{V_c^2-V^2}{gI_{sp}EpV}\right)^2 E\right)\frac{1}{u'}\frac{du'}{d\alpha}\right.$$
$$\left. - \left(\frac{V_c^2-V^2}{gI_{sp}EpV}\right)^2\frac{G}{Ep}\frac{dEp}{d\alpha}\right] \tag{A5}$$

where

$$A = \sum_{k=1}^{\infty}\frac{(-1)^k}{(2k)!}\sum_{j=2k+1}^{\infty}\frac{2k-j}{j}(u'm_n)^{2k-j}(u^j - u_0^j)$$

$$B = \sum_{k=1}^{\infty}\frac{(-1)^k}{(2k)!}\sum_{j=2k+1}^{\infty}(u'm_n)^{2k-j}(u^{j-1} - u_0^{j-1})$$

$$C = u'(m_0\cos[u_0] - m\cos[u]) - \sin(u_0) - \sin(u)$$

$$D = \sum_{k=1}^{\infty}\frac{(-1)^k}{(2k)!}\sum_{j=2k+1}^{\infty}(u'm_n)^{2k-j}u^{j-1}(u-u_0)$$

$$E = u'm_0(\sin[u_0] - \sin[u])$$

$$F = u'm(u_0-u)\cos(u)$$

$$G = u'(m_0\sin[u_0] - m\sin[u]) - \cos(u_0) + \cos(u)$$

References

[1]Hoge, H.J. and Rudiger, T.P., "Concept Evaluation of a Maneuverable Reentry Research Vehicle (MRRV) and Related Experiments," AFWAL-TR-81-3125, Nov. 1981.

[2]Limerick, C.D. and Cuffe, J.P.B., "Propulsion for an Air-Launched Space Sortie System," AFRPL-TR-82-069, Vols. I to III, Dec. 1982.

[3]Ehrlich, C.F. Jr. et al., "Advanced Military Spaceflight Capability (AMSC) Technology Identification Study, AFWAL-TR-83-3055, 1983.

[4]General Dynamics, "Advanced Military Spaceflight Capability Technology Identification Study," General Dynamics Final Review, Contract F33615-81-C-3019, San Diego, Calif., Mar. 1983.

[5]Cuadra, E. and Arthur, P.D., "Orbit Plane Change by External Burning Aerocruise," *Journal of Spacecraft and Rockets*, Vol. 3, March 1966, pp. 347-352.

[6]Lau, J., "Implications of Maneuvering-Range Constraints on Lifting Vehicle Design," *Journal of Spacecraft and Rockets*, Vol. 4, May 1967, pp. 639-643.

[7]Clauss, J.S., Jr. and Yeatman, R.D., "Effect of Heating Restraints on Aeroglide and Aerocruise Synergetic Maneuver Performance," *Journal of Spacecraft and Rockets*, Vol. 4, Aug. 1967, pp. 1107-1109.

[8]Dickmanns, E.D., "The Effect of Finite Thrust and Heating Constraints on the Synergetic Plane Change Maneuver for a Space Shuttle Orbiter-Class Vehicle," NASA TN-D-7211, Oct. 1973.

[9]Joosten, B.K. and Pierson, B.L., "Minimum Fuel Aerodynamic Orbital Plane Change Maneuvers," AIAA Paper 81-0167, AIAA 19th Aerospace Sciences Meeting, St. Louis, Missouri, Jan. 1981.

[10]Hull, David G., "Optimal Reentry and Plane-Change Trajectories," Paper 81-156, AAS/AIAA Astrodynamics Specialist Conference, Lake Tahoe, Nev., Aug. 1981.

[11]Ikawa, H. and Rudiger, T.F., "Synergetic Maneuvering of Winged Spacecraft for Orbital Plane Change," *Journal of Spacecraft and Rockets*, Vol. 19, Nov.-Dec. 1982, pp. 513-520.

[12]London, H.S., "Change of Satellite Orbit Plane by Aerodynamic Maneuvering," *Journal of Aerospace Sciences*, Vol. 29, No. 3, Mar. 1962, pp. 323-332.

[13]Nyland, F.S., "The Synergetic Plane Change for Orbiting Spacecraft," Memorandum No. RM-3231-PR. The Rand Corporation, Santa Monica, Calif., Aug. 1962.

[14]Parsons, W.D., "Analytic Solution of the Synergetic Turn," *Journal of Spacecraft*, Vol. 3, No. 11, Nov. 1966, pp. 1675-1678.

[15]Koelle, H.H., ed., *Handbook of Astronautical Engineering*, first ed., McGraw-Hill Book Company, Inc., New York, 1961, pp. 8-21.

[16]Bate, R.R., Mueller, D.D., and White, J.E., *Fundamentals of Astrodynamics*, Dover Publications, Inc., New York, 1971, pp. 396-407.

[17]Selby, S.M., ed., *Standard Mathematical Tables*. 20th ed., The Chemical Rubber Co. Press, Cleveland, Ohio, 1972, p. 397.

[18]Brauer, G.L., Cornick, D.E., and Stevenson, R., "Capabilities and Applications of the Program to Optimize Simulated Trajectories (POST)," NASA CR-2770, Feb. 1977.